

# DESIGN AND RELIABILITY OF CERAMIC COMPONENTS FOR AUTOMOTIVE APPLICATIONS

V. Knoblauch<sup>1</sup>, R. Speicher<sup>1</sup> and G.A. Schneider<sup>2</sup>

<sup>1</sup> Robert Bosch GmbH, Dep. FV/FLW, 70049 Stuttgart, Germany

<sup>2</sup> Technical University Hamburg-Harburg, Advanced Ceramics Group, 20173 Hamburg-Harburg, Germany

## ABSTRACT

In this paper a holistic design approach for structural ceramic components is demonstrated for a valve plate of  $\text{Si}_3\text{N}_4$  used in high pressure pumps for diesel injection systems, such as Common Rail Direct Injection. In order to realize low fuel consumption and low exhaust gas emission a high injection pressure is required. However, pressures of up to 1600 bar make great demands on the materials used. In addition, reliability requirements in automotive are quite ambitious. Thus, the use of ceramic components in these systems needs a high factor of safety. This requires a detailed characterization of the material properties as well as extensive calculations of mechanical stressing, failure probability and lifetime.

Finite Elements calculations prior to lifetime considerations are done in order to investigate the stress states during cyclic loading. For calculations of failure probability and lifetime the Finite Element post processor STAU [1] is used taking into account the Weibull-distribution of the materials strength as well as fatigue under static and cyclic loading. 4-point-bending strength as well as results from valve plate tests are presented. Static and cyclic subcritical crack growth parameters are investigated in bending technique as well. Three different material suppliers of commercial  $\text{Si}_3\text{N}_4$  are evaluated. Finally, a proof test will be presented to ensure the demanding quality standards.

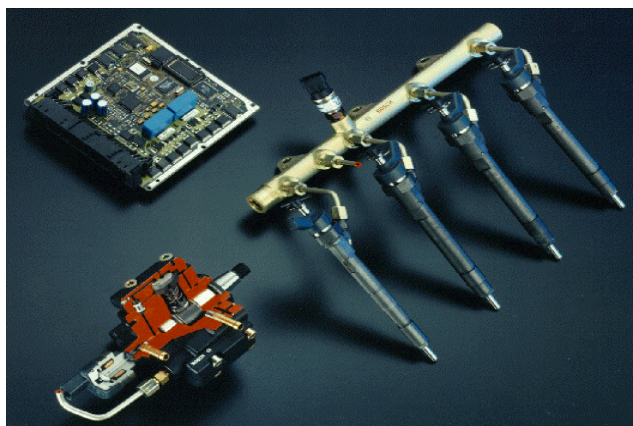
## 1. INTRODUCTION

Ceramic materials are offering various attractive characteristics for automotive applications such as high temperature resistance, wear and corrosion resistance and low density. However they are quite brittle and fail spontaneously almost without any plastic deformation. Voids caused by production which are predominantly present in the specimens volume and voids from surface grinding are failure origins. These voids are different in shape, length and orientation to principal stresses, which results in a large scatter in strength. Thus, a statistical approach is required as well as convenient and reliable methods to determine materials data. For the evaluation of strength data it is important to know which specimen type has to be used. Often, data from standard specimens do not characterize the failure behavior of the component properly. In such cases the component itself has to be investigated.

In the first part of the paper the mounting of the component within the injection system and the loading situation is described. Furthermore, finite element simulations of the mechanical stressing are shown. Subsequently, material properties of three different types of  $\text{Si}_3\text{N}_4$  derived from standard test specimen and component tests are presented. In the reminder of the paper these data are used to carry out calculations of failure probability and lifetime as well as to develop a proof test concept.

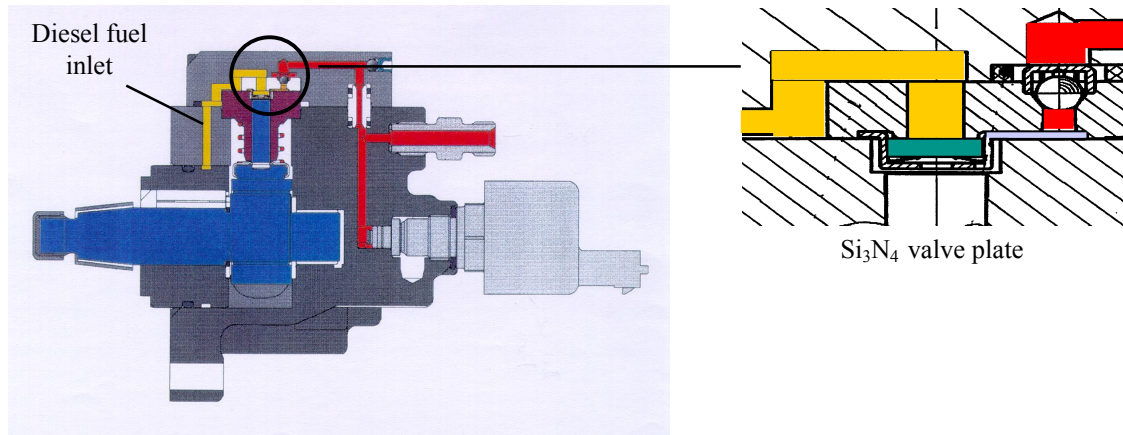
## 2. COMMON-RAIL INJECTION PUMPS

Recently, there is an increasing interest in improving the performance of direct-injection automotive diesel engines, in order to reach low emissions of  $\text{NO}_x$  and low fuel consumption. Common-Rail systems offer a large variability to improve these parameters, e.g. mass flow, pilot injection, injection time.



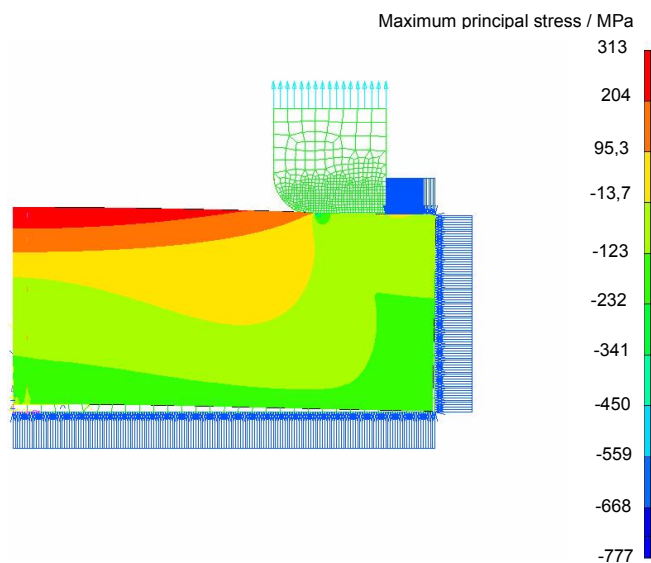
**Figure 1.** Common-Rail injection system, including high-pressure pump, rail, injectors and electronic control unit

Fig. 1 shows the Common-Rail injection system including high-pressure pump, rail, injectors and control device. The pump generates a maximum pressure of about 1350 bar, which is led via the rail to the injectors. The rail offers the advantage of acting as a pressure reservoir which provides a constant pressure during the whole injection period. The control device governs the pump and the injectors. The high-pressure pump with the valve plate made of  $\text{Si}_3\text{N}_4$  which operates as an inlet valve is shown more detailed in fig. 2.



**Figure 2.** High-pressure pump with detailed view of the cylinder head including valve plate

When the piston goes downwards, the existing depression opens the valve plate until it is constrained by a cage, which can not be modified because of the compression cycle. For high performance it is very important that the cylinder is filled totally with fuel while the piston moves downwards. Therefore, the thickness of the valve plate has to be as small as possible. The aim of all investigations presented here is to determine the smallest thickness for reliable operation.



**Figure 3.** FE analysis of the valve plate at 1420 bar. Used materials data: valve plate  $E = 300 \text{ GPa}$ ,  $\nu = 0.26$   
housing: elast.-plast. material behavior  $E = 207 \text{ GPa}$ ,  $R_{es} = 800 \text{ MPa}$ ,  $R_m = 1200 \text{ MPa}$

Fig. 3 shows the FE model of the valve plate including housing for a plate thickness of 1.4 mm and a plate diameter of 6 mm. The applied pressure is 1420 bar due to the maximum error of 70 bar in the pressure sensor. The analysis is done with the FE code ABAQUS using the surface-based contact algorithm. Axisymmetric elements are used with an element size of 0.02 mm at the contact areas. A friction coefficient of 0.2 is used. A variation to 0.5 did not result in a difference in the resulting stresses. The resulting biaxial stresses exhibit maximum of 313 MPa at the center of the tensile surface of the valve plate.

### 3. MATERIALS DATA

In order to carry out calculations of reliability, strength and subcritical crack growth data have to be determined. For measurements of strength, both 4-point bending tests and valve plate tests have been performed because the influence of specimen geometry and surface condition has to be taken into account. However, static and cyclic fatigue tests are carried out using 4-point bending tests only. It is assumed that the fatigue behavior is less influenced by specimen shape and surface conditions (as long as they are comparable in quality).

#### 3.1. Strength measurements

4-point bending measurements were carried out according to DIN EN 843-1 [2]. The cross-section of the specimens was 3 x 4 mm. An inner load span of 20 mm and an outer load span of 40 mm were used. The velocity of loading was 5 mm/min, which resulted in fracture of the specimens after less than 10 s.

The valve plate tests have been performed using a special kind of ring-on-ring test adapted to the dimensions of the valve plate. The supports are made of WC/Co-hard material (1800 HV30) with a Young's modulus of 640 GPa and a Poisson's ratio of 0.22. The bending strength is about 3100 MPa. A finite element analysis of the stress distribution is shown in fig. 4.

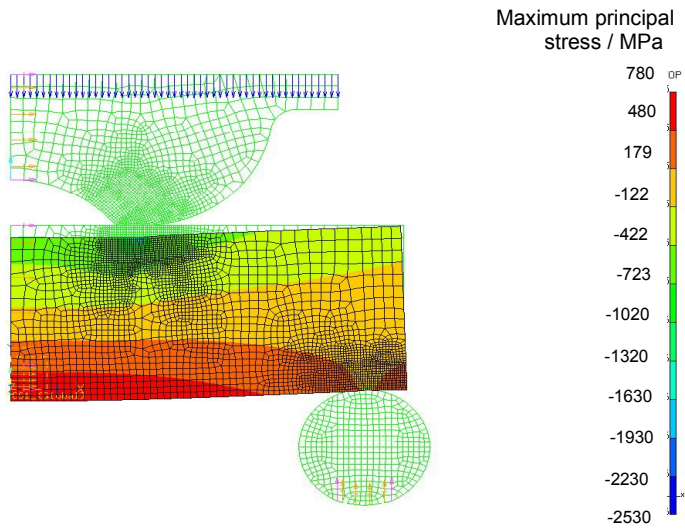


**Figure 4.** FE analysis of the valve plate test. Materials data of the housing:  $E = 640$  GPa,  $\nu = 0.22$

Three different material suppliers using different shaping and sintering procedures have been examined. Two material qualities were axially pressed, the other supplier used an injection molding process. The sintering process is done by gas pressure or hot isostatic pressing procedures. All these materials are commercially available.

In order to compare 4-point bending data and valve plate data, the effective volume of the specimens has to be taken into account. Therefore, the size effect has to be considered, according to:

$$\sigma_{0,\text{corr}} = \sigma_{0,\text{valve plate}} \cdot \left( \frac{V_{\text{eff, valve plate}}}{V_{\text{eff, 4-point}}} \right)^{\frac{1}{m}} \quad (1)$$

In equation (1)  $V_{\text{eff, valve plate}}$  is the effective volume of the valve plate in the valve plate test, and  $V_{\text{eff, 4-point}}$  the effective volume of the 4-point bending bar.  $\sigma_{0,\text{valve plate}}$  and  $m$  are the Weibull parameters obtained from a Weibull evaluation using the Maximum likelihood method [3].  $\sigma_{0,\text{corr}}$  is the strength level of the valve plate calculated for the effective volume of 4-point bending bars. This value can be compared with the Weibull parameter  $\sigma_0$  of 4-point bending tests.  $V_{\text{eff, valve plate}}$  and  $V_{\text{eff, 4-point}}$  are calculated using STAU, where the orientation of flaws is considered. Therefore, analytical solutions for  $V_{\text{eff, 4-point}}$ , e.g. given in [3], cannot be used. The results are shown in fig. 5. It is obvious that for all materials the characteristic strength  $\sigma_0$  of 4-point bending tests is higher than the strength derived from valve plates. However, for material C the smallest difference is obtained. That means that the material supplier C fits best the strength level of bending bars and valve plates.

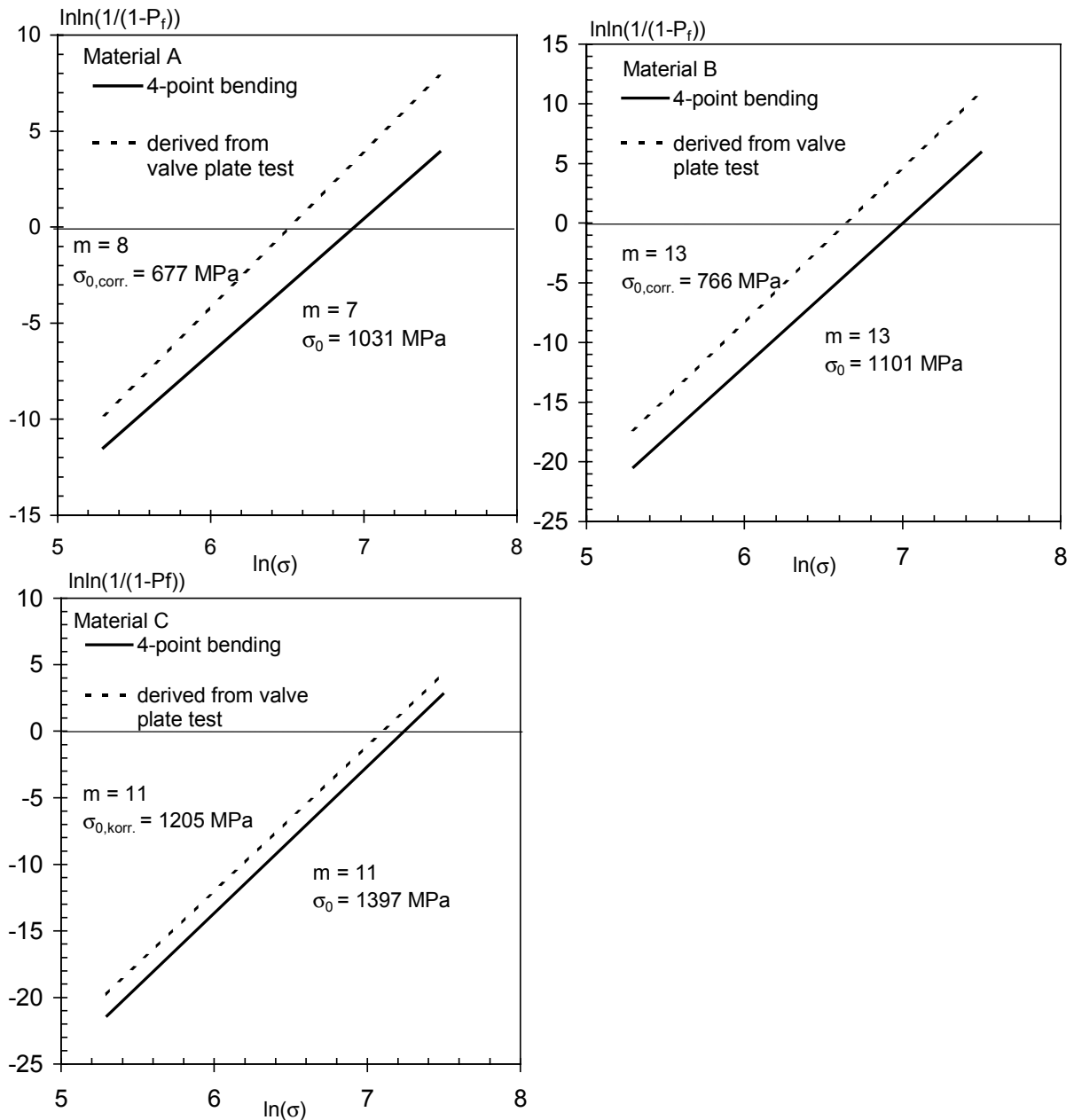


**Figure 5.** Results of strength investigations in 4-point bending tests compared with values derived from valve plate tests. Comparison between different material suppliers.

### 3.2. Subcritical crack growth measurements

Static and cyclic fatigue tests were performed using 4-point bending techniques. To evaluate v-K-curves the modified lifetime method proposed by Fett [4, 5] has been used. For the calculation of the reliability of valve plates during cyclic loading in the high-pressure pump, no static experiments would be necessary. However, to check cyclic fatigue effects both tests have been done.

For static tests a maximum loading time of 500 h was chosen. The probability of spontaneous failure was set to a maximum of 10 % except for material A, where the low Weibull modulus led to a higher failure probability. The cyclic fatigue tests were done at  $R = 0.2$ . In the application a stress ratio of  $R = 0$  will occur. But the chosen ratio of  $R = 0.2$  enables an easier experimental set-up. The frequency in the high-pressure pump reaches a maximum value of 50 Hz. However, the resonance-frequency testing machine used necessitated a frequency of 78 Hz. The relation for static subcritical crack growth has to be written as a power law according to:

$$v = \frac{da}{dt} = A^* \cdot \left( \frac{K_I}{K_{Ic}} \right)^n \quad (2)$$

and respectively for cyclic loading:

$$v = \frac{da}{dt} = f \cdot \frac{da}{dN} = A^* \cdot \left( \frac{K_{I,max}}{K_{Ic}} \right)^n \quad (3)$$

The results are shown in table 1. Material A exhibits very low n values for static and cyclic fatigue which are of interest for lifetime calculations. However, the difference between static and cyclic loading is very small. For Material B a large difference between static and cyclic n values was obtained. That means, that there is a cyclic fatigue effect. The result of material C is quite surprising since the cyclic fatigue parameter n is larger than the static one. It has to be mentioned that the evaluation of parameters of subcritical crack growth has some uncertainties as revealed in [6].

**Table 1.** Parameters of subcritical crack growth from static and cyclic bending tests

Material	$n_{stat}$	$A^*_{stat}$ m/s	$n_{cycl}$	$A^*_{cycl}$ m/s
A	27	$3.2 \cdot 10^{-8}$	22	$1.6 \cdot 10^{-7}$
B	47	$8 \cdot 10^{-4}$	24	$2 \cdot 10^{-5}$
C	35	$4 \cdot 10^{-8}$	38	$1.2 \cdot 10^{-7}$

In order to evaluate if the determination of subcritical crack growth in 4-point bending techniques is valid for valve plates, cyclic fatigue investigations of valve plates have been performed using a similar experimental set-up as shown in fig 4. A radial fixation of the specimens prevented a sliding motion during cyclic loading. The tests were carried out at 84 Hz using a resonance-frequency machine which counted the cycles until failure. A statistical evaluation of these numbers of cycles together with the Weibull modulus of the inert strength distribution reveals the parameters of subcritical crack growth. Using a least square fit,  $n = 27$  and  $A^* = 1.2 \cdot 10^{-5}$  m/s is found for material B which is in very good agreement with data from cyclic 4-point bending tests.

#### 4. CALCULATIONS OF RELIABILITY

##### 4.1. Failure probability

Stress analysis of the components using finite element method in combination with reasonable materials data provide the basis for calculations of reliability. Ziegler [7] has expanded the existing models for the calculations of failure probability for cyclic periodic loadings. It leads to the failure probability  $P_f$  as a function of cycles N:

$$P_f(N) = 1 - \exp \left[ - \frac{1}{V_0} \int_V dV \frac{1}{4\pi} \int_{\Omega} d\Omega \left( \frac{\sigma_0^2}{B} \cdot N \cdot \int_0^T \left( \frac{\sigma_{eq}(t)}{\sigma_0} \right)^n dt \right)^{\frac{m}{n-2}} \right] \quad (4)$$

In equation (4), V is the component volume,  $V_0$  a reference volume,  $d\Omega$  represents the consideration of flaw orientation,  $\sigma_0$  and m are Weibull parameters of the inert strength distribution and n and B are the parameters of subcritical crack growth at cyclic loading. B and  $A^*$  are linked with equation (5)

$$B = \frac{2}{A^* \cdot Y^2 \cdot (n-2)} K_{Ic}^2 \quad (5)$$

Y was chosen to be 1,99 according to very small cracks in 4-point bending [8]. T is the period time of one cycle. It has to be mentioned that  $\sigma_{eq}$  is a function of time and equation (4) is only correct for periodic stresses [7]:

$$\sigma_{eq}(t+T) = \sigma_{eq}(t) \quad (6)$$

The results for all three materials are shown in table 2. It should be mentioned that the Weibull parameter derived from investigations of valve plates have been included in the calculations. As shown, only material C does not exceed the maximum acceptable failure probability of  $1 \cdot 10^{-6}$ .

**Table 2.** Failure probability of valve plates after  $4 \cdot 10^8$  cycles for materials A, B and C including used material data. Comparison with two virtual combinations.

Material	m	$\sigma_0$ MPa	$n_{cycl}$	$A^*_{cycl}$ m/s	$P_f$ ( $N=4 \cdot 10^8$ )
A	8	677	22	$1.6 \cdot 10^{-7}$	$> 1 \cdot 10^{-2}$
B	13	766	24	$2 \cdot 10^{-5}$	$> 1 \cdot 10^{-3}$
C	11	1205	38	$1.2 \cdot 10^{-7}$	$< 1 \cdot 10^{-6}$
Combination 1	11	766	38	$1.2 \cdot 10^{-7}$	$1.27 \cdot 10^{-4}$
Combination 2	11	1205	24	$2 \cdot 10^{-5}$	$8.5 \cdot 10^{-5}$

To investigate the influence of materials data, m,  $n_{cycl}$  and  $A^*_{cycl}$  from material A and  $\sigma_0$  from B was used for a calculation (combination 1, see table 2). The difference between combination 1 and material C is larger than  $10^2$ . Using the inert strength data of material C and the subcritical crack growth data from B (combination 2) results in the difference of approx.  $10^2$  related to material C. Hence, for this cyclic calculation, both strength data and subcritical crack growth data have similar influence on the failure probability.

#### 4.2. Proof test

As shown in table 2, materials A and B do not fulfill the required survival probability. Thus, a proof test of the valve plates has been introduced. In a proof test all components are stressed with a load higher than the load during operation. Components which would fail during real operation will fail spontaneously during proof testing. It is obvious that the stress state under proof test loading should be very comparable to the real loading situation. Furthermore, the stressing has to take place quite fast to avoid subcritical crack growth. In our case, the modified ring-on-ring supports shown in fig. 4 were used. A comparison of the stress distribution at the tensile surface in both loading conditions shows a very good coincidence.

For the calculation of proof test ratios equation (7) is used:

$$\left( \frac{\sigma_p}{\sigma} \right) = \left( \frac{\sigma^2 \cdot t_{B,min}}{B} \right)^{\frac{1}{n-2}} \quad (7)$$

n and B are parameters of subcritical crack growth under cyclic loading conditions,  $\sigma$  the stress of the valve plate in the high-pressure pump,  $\sigma_p$  the maximum stress of the valve plate during proof testing and  $t_{B,min}$  the operation time of the pump without failure of the valve plate.

The result for a valve plate thickness of 1.4 mm is shown in fig. 6. It can easily be seen that for lower values of n the proof test ratio is more influenced by the parameter  $A^*$  than for high values of n.

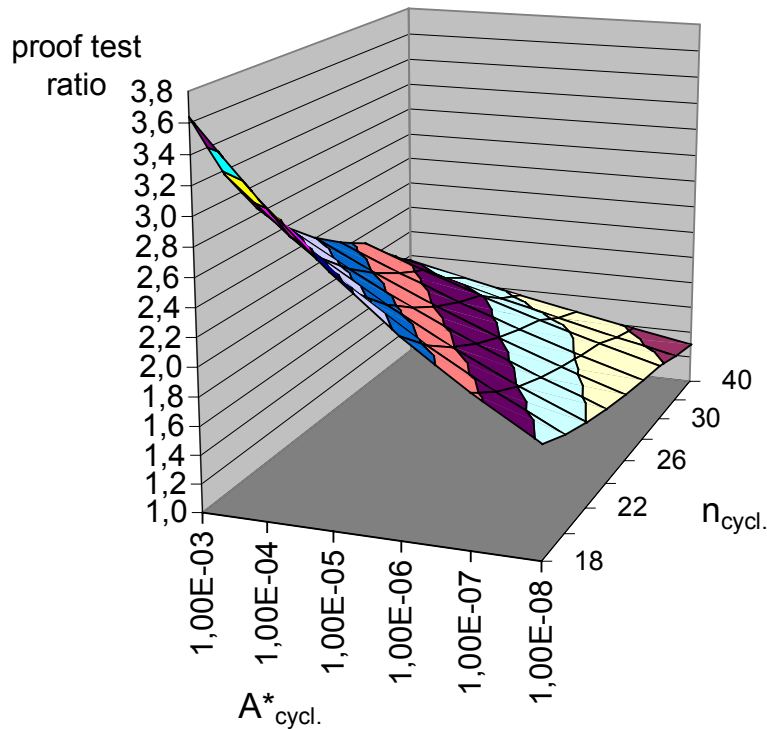


**Figure 6.** Proof test ratio for valve plates with thickness of 1.4 mm using cyclic subcritical crack growth parameters

## 5. SUMMARY AND DISCUSSION

Calculations of failure probabilities using the finite element post processor STAU are demonstrated for a cyclic loaded valve plate made of  $\text{Si}_3\text{N}_4$  which is used in Common-Rail high-pressure injection pumps. Three different materials of commercial suppliers have been investigated.

It is shown that inert strength measurements of valve plates have to be used, because 4-point bending results do not match the strength distribution of valve plates. The Weibull modulus was between 7 and 13, the characteristic strength derived from valve plate tests and calculated for the effective volume of 4-point bending bars was between 677 and 1205 MPa.

Parameters of subcritical crack growth are determined under static cyclic conditions using 4-point bending techniques. Static  $n$  values ranged from 27 to 47, cyclic values from 22 to 38. For one material, cyclic fatigue tests of valve plates were performed. A very good agreement with the results of 4-point bending bars was obtained.

Calculations of failure probabilities after  $4 \cdot 10^8$  cycles showed that two materials exceed the tolerable failure probability of  $1 \cdot 10^{-6}$ . They reached failure probabilities after operation time of about  $1 \cdot 10^{-2}$ . Therefore, proof testing procedures were investigated. Proof test ratios up to a factor of two are necessary for reliable operation of the valve plates in high-pressure pumps.

Further investigations have to be done examining the influence of R-curve behavior. Toughening mechanisms necessitate to modify  $K_I$  in equation (2) according to:

$$K_{I,\text{tip}} = K_{I,\text{appl}} + K_{I,\text{sh}} \quad (K_{I,\text{sh}} < 0) \quad (8)$$

A hint of existing R-curve behavior may be the difference between static and cyclic  $n$  value of subcritical crack growth of material B. Crack bridging of elongated grains is subject to cause R-curve behavior. These crack bridges are destroyed during cyclic loading, which results in the low  $n$ -values obtained.

## References

1. A. Heger, in Fortschritt-Berichte VDI, Reihe 18, Nr. 132, VDI-Verlag Düsseldorf, Germany, 1993
2. DIN EN 843-1, Monolithische Keramik, Mechanische Eigenschaften bei Raumtemperatur, Teil 1: Bestimmung der Biegefestigkeit, Deutsches Institut für Normung, Berlin, Germany, 1995
3. D. Munz, T. Fett: Ceramics, Mechanical properties, failure behaviour, Materials Selection, Springer Verlag Berlin, Germany, 1999
4. T. Fett, D. Munz, J. Am. Ceram. Soc., Vol 68, 8, C-213 – C-215, 1985
5. T. Fett, G. Martin, D. Munz, G. Thun, J. of Materials Science, 26, 3320 – 3328, 1991
6. H. A. Lindner, B. Caspers in Mechanische Eigenschaften keramischer Konstruktionswerkstoffe (Ed.: G. Grathwohl), Verlag DGM Informationsgesellschaft, Oberursel, Germany, 1993, Chapter V, 191 – 195
7. Ch. Ziegler, in Fortschritt-Berichte VDI, Reihe 18, Nr. 238, VDI-Verlag Düsseldorf, Germany, 1998
8. Draft of DIN 51109, Testing of advanced technical ceramics, determination of fracture toughness  $K_{Ic}$ , Deutsches Institut für Normung, Berlin, Germany, 1991